Journal of Molecular Graphics and Modelling 35 (2012) 11–20

Contents lists available at SciVerse ScienceDirect

Journal of Molecular Graphics and Modelling

journal homepage: www.elsevier.com/locate/JMGM

Microsolvation and hydrogen bond interactions in Glycine Dipeptide: Molecular dynamics and density functional theory studies

Balasubramaniam Yogeswari [a], Ramasamy Kanakaraju [a], Subramaniam Boopathi [b], Ponmalai Kolandaivel [b,*]

[a] Department of Physics, NGM College, Pollachi 642 001, India
[b] Department of Physics, Bharathiar University, Coimbatore 641 046, India

ARTICLE INFO

Article history:
Received 2 December 2011
Received in revised form 10 February 2012
Accepted 13 February 2012
Available online 20 February 2012

Keywords:
Glycine Dipeptide
Microsolvation
AIM analysis
Natural bond orbital
NMR

ABSTRACT

Molecular dynamics (MD) simulations were carried out to study the conformational characteristics of Glycine Dipeptide (GD) in the presence of explicit water molecules for over 10 ns with a MD time step of 2 fs. The density functional theory (DFT) methods with 6-311G** basis set have been employed to study the effects of microsolvation on the conformations of GD with 5–10 water molecules. The interaction energy with BSSE corrections and the strength of the intermolecular hydrogen bond interactions have been analyzed. The Bader's Atoms in Molecules (AIM) theory has been employed to investigate H-bonding patterns in water interacting complexes. The natural bond orbital (NBO) analysis has been carried out to analyze the charge transfer between proton acceptor to the antibonding orbital of the X—H bond in the hydrated complexes. NMR calculations have been carried out at B3LYP/6-311G (2d, 2p) level of theory to analyse the changes in structure and hydrogen bonding environment that occur upon solvation.

1. Introduction

The hydrogen bond interactions play a key role in determining shapes, properties and functions of biomolecules [1] particularly in the formation and stabilization of protein secondary structure [2]. Theoretical calculations of complexes between biomolecules and environmental molecules such as ligands and solvent molecules are promising for medicine, biotechnology and provide deeper insight into functioning of biosystems [3,4]. In addition to the prevalence within proteins, the characteristic properties of water molecule which has ability to act as hydrogen bond donor and acceptor lead to a strong preference of water as a solvent for biomolecules [5]. Water molecules which are integral part of functioning of biological systems interact with biomolecules by forming intermolecular hydrogen bonds [6]. Many studies have illustrated the unique role of water in the conformations of biomolecules [7,8]. The role of solvent in deciding the conformational preferences of biological molecules is now well known and attributable to microsolvation [9,10] which refers to the chemical environment in which a solute molecule is surrounded by a definite number of water molecules in a specific configuration held together by hydrogen bonds. In solvated environments, small molecules such as peptides provide an excellent vehicle to get significant insights to structure, solvation and of larger effects like protein folding. Considering the role of hydrogen bonding in protein folding, finding potential markers for tracking the peptide bond hydrogen bonding state is of great importance. MD simulation studies [11] have also contributed to the view that water plays a crucial role in mediating protein dynamics at the molecular level [12].

Glycine Dipeptide (GD), a paradigm to study the peptide–water interaction provides valuable information regarding the hydration of proteins. The interaction between peptides and water molecules have been studied extensively both experimentally [5,13–18] and theoretically [19–25]. The crystal structure of GD was determined by Kameda et al. [13] and they have found that the GD-hydrate crystal has three water molecules per two molecules of dipeptide. Sieler et al. [14] have measured the spectra for the amide bond of GD and N-acetylglycine in water, and analyzed the dynamics of atoms in an aqueous environment. Liu et al. [15] have experimentally investigated the non covalent interactions between the dialanine and diglycine peptides and water molecules and aggregation between two peptide molecules through AMBER simulations followed by a DFT optimization. Bhate et al. [16] have investigated experimentally and theoretically the structure and solvation of the four alanine and glycine containing dipeptides by measuring the ^{13}C and ^{15}N NMR chemical shift values. Born et al. [17] reported the ability to detect the onset of collective network motions in model peptides, as a function of solvation, using terahertz spectroscopy. Fischer et al. [18] have measured the infrared absorption

* Corresponding author. Tel.: +91 422 2428441; fax: +91 422 2422387.
E-mail address: ponkvel@hotmail.com (P. Kolandaivel).

1093-3263/$ – see front matter © 2012 Elsevier Inc. All rights reserved.
doi:10.1016/j.jmgm.2012.02.002

spectra of glycine and its dipeptide using a novel spray-sampling technique.

Abramov et al. [19] have studied the intermolecular hydrogen bond interactions in glycylglycine dimer. The importance of electron correlation effects in the peptide bond formation in GD is investigated by Chaudhuri et al. [20] by using ab initio and DFT methods. Selvarengan et al. [21] have theoretically studied the intermolecular hydrogen bond interactions in the monohydrated complexes of formamide, N-methylacetamide and GD. Makshakova et al. [22] have investigated the optimized geometries and interaction energies of the complexes between α-helical polypeptides, poly-L-alanine, poly-L-glutamic acid, poly-L-benzyl-glutamate and a single water molecule through molecular mechanics, semi empirical and DFT methods. Hugosson et al. [23] have made a comparative theoretical study of the glycine–alanine dipeptide in water and concluded that the solvation pattern differ substantially for carboxy and aminoterminii and the backbone amid NH group. The strength of H-bond formed between GD and water molecule as acceptor is assessed by Scheiner [24] who documented that even in the absence of any external geometric constraints, the potential strength of a peptide containing H-bonds is rather sensitive to the internal conformation of the peptide. Keefe et al. [25] tried to unlock the mysteries of protein folding problem using ab initio methods to examine the precise structural features of the peptide bond in a series of peptides including alanylglycine dipeptide. Elmi et al. [26] have studied the intermolecular hydrogen bonds of α-glycylglycine in its crystalline phase using ab initio calculated ^{14}N and ^{2}H nuclear quadrupole coupling constants. Scheiner [27] monitored the structural and spectroscopic features of the GD which is paired with one or more formamide molecules via ab initio calculations and analyzed the perturbations induced by a CH···O H-bond between the dipeptide and formamide. Yan et al. [28] have investigated the effect of glycyl dipeptides (glycylglycine, glycyl-L-valine, and glycyl-L-leucine) on the micellar properties of gemini surfactant pentamethylene-1,5-bis (dodecyldimethylammonium bromide) by means of conductivity and fluorescence spectroscopy. The results obtained by conductivity show that the effect of glycyl dipeptides depends upon their nature and concentration, as well as the temperature. Cheam [29] studied the ab initio force field of GD at 4–21 level for a conformation close to that in the crystal and with four intermolecular H-bonds provided by four water molecules. With these backgrounds, our present study aims to gain more knowledge about the impact of solvent molecules on the conformational characteristics of GD. MD simulations over the 10 ns time scale was performed with a focus on radial distribution function and water shell analysis. In addition, the B3LYP and B3PW91 density functional theory (DFT) methods are used to study the stepwise hydration of the five lowest energy conformers of GD with 5–10 water molecules. Since the solvation effect of one to four water molecules is less significant, we have initiated our study from 5 water molecules. This study was started with an aim to construct a hydration shell with 11 water molecules around all the five lowest energy conformers of GD, but, due to steric hinderance, all the conformers of hydrated GD fail to converge except GDC4. Hence, we have reduced the number of water molecules to 10 and the hydration positions were selected to enable maximal hydrogen bonding between water and GD and between water molecules. In addition, the H-bonding ability of the GD conformers with water molecules has also been investigated. The initial geometry optimization was performed on GD, starting from the known crystal structure [13]. The possible minimum energy conformers of GD have been obtained through the potential energy surface (PES) scan for the main chain dihedral angles ψ (N—C—C^{α}—N) and φ (C—N—C^{α}—C) with an incremental step size of 30° at B3LYP/6-311G** level of theory.

2. Computational details

The optimized structure at B3LYP/6-311G** level of theory was immersed in the TIP3P water model box of 32.85 Å × 29.98 Å × 28.18 Å with 576 water molecules. With periodic boundary conditions, the simulation was carried out over 10 ns time scale at constant pressure. Initially, the system was subjected to a geometry relaxation by using the steepest descent algorithm. The system was subjected to 20 ps equilibrium process in which the temperature was gradually raised from 0 to 300 K under the atomic restraints of 10 kcal/mol and made suitable for MD simulation run. The langevin dynamics (NTT = 3) were used to control the temperature at 300 K, with a collision frequency of 1.5 ps^{-1}. As TIP3P water [30] model is found to be well balanced with the Amber force field [31], it was used here for water modeling. All the simulations were performed with Amber 8.0 program package [32] using ff03 force field.

In quantum chemical calculations, the density functional theory (DFT) with Becke's three parameter exact exchange functional (B3) [33] combined with gradient-corrected Lee–Yang–Parr correlation functional (LYP) [34] and Perdew and Wang's 1991 (PW91) [35] have been employed to predict the structure, molecular properties and stability of the five lowest energy conformers of GD and their hydrated complexes using 6-311G** basis set. The vibrational frequency analysis has been performed to confirm the minimum energy structures. The H-bond interaction energy which is the energy of interaction of all the separated molecules in the solvated complexes have been corrected for the basis set superposition errors (BSSE), using the counterpoise method of Boys and Bernardi [36] using the equation

$$E_{\mathrm{int}}(\mathrm{corr}) = E_{\mathrm{AB}}(\mathrm{AB}) - [E_{\mathrm{A}}(\mathrm{AB}) + E_{\mathrm{B}}(\mathrm{AB})] \quad (1)$$

where E_{AB}(AB) is the energy of the complex, E_{A} (AB) and E_{B} (AB) are the energies of monomers A and B with full complex basis set by setting the appropriate nuclear charge to zero, which is located at the same intermolecular configuration as in the complex. The AIM calculations were performed at B3LYP/6-311G** level of theory based on Bader's and co-workers approach [37]. The NBO analysis has also been carried out for the water interacting complexes using the same level of theory. It is used to obtain information on the changes of electron densities in proton donor and proton acceptor, as well as the changes in the bonding and anti-bonding orbitals. For each donor NBO (i) and acceptor NBO (j), the stabilization energy $E^{(2)}$ associated with $i \rightarrow j$ is given by

$$E^{(2)} = q_i \frac{F^2(i,j)}{\varepsilon_i - \varepsilon_j} \quad (2)$$

where q_i is the orbital occupancy of the ith donor, ε_j, ε_i are diagonal elements (orbital energies) and $F(i, j)$ is off diagonal elements associated with NBO Fock matrix. In order to get a sense of the GD conformations stabilized in the solvated state and to find out the sensitivity of the chemical shift values to the changes in structure and hydrogen bonding, the NMR calculations have been carried out for all the structures based on the Cheeseman et al. [38] method at B3LYP/6-311G (2d, 2p) level of theory. All the above calculations were performed using the Gaussian 03W program [39].

3. Results and discussion

3.1. Molecular dynamics

The details of the system used for simulation is given in Table 1. The conformational changes of GD in the vicinity of water environment around 10 ns are shown in Fig. 1. During simulation, the GD fluctuates a lot which may be due to its interaction with surrounding aqueous solution. Knowing the strength of H-bond in linking

Table 1
Simulation set-up prepared to run molecular dynamics for GD.

Solute	Force field	No. of water molecules	Volume of the simulation box (Å^3)	Solvent	Simulation length (ns)	Temperature (K)
GD	Leaprcff03	576	27752.88	H_2O	10	300

the protein structures particularly in water environment is important in predicting the activity of proteins such as protein folding and protein binding energy [12,40]. The H-bond analysis shows that the oxygen (O), nitrogen (N) and carbon (C) atoms of GD are found to interact with the water molecules as hydrogen bond donors.

The radial distribution function analysis (see Fig. 2) shows that the first co ordination shell is characterized by a major peak at around 1.85 Å for O(GD)···H(W). Fig. 3 shows the number of water molecules that occupy the first and second solvation shell of GD. An average of two water molecules is often found to interact with distances ranging from 2.2 to 3.6 Å. At times (around 343.5 ps), four water molecules are found to interact with GD residues. On the other hand, nearly 52–58 water molecules occupy the second solvation shell with distances ranging from 3.6 to 6.0 Å. These water molecules do not interact directly with GD residue but they also contribute to some extend on the conformation of GD. The ratio $g_{max}^{O-H}/g_{min}^{O-H}$ [41] can be used as a criterion to establish the strength of the hydrogen bonding interaction between the O(GD)···H(W) pairs, where the values of $g_{max}^{O_{GD}-H_W}/g_{min}^{O_{GD}-H_W} = 3.0936$. The H-bond formed between the C(GD)···H(W) at 4.45 Å with H-bond strength of $g_{max}^{O_{GD}-H_W} = 1.1844$ clearly indicates that the carbon atoms has negligible contribution to the conformational change in GD. The H-bond strength is found to be O(GD)···H(W) > C(GD)···H(W) > N(GD)···H(W).

3.2. Quantum chemical studies

3.2.1. Structure and energy

The optimized structures of the most stable hydrated complexes of GD with 5–11 water molecules at B3LYP/6-311G** level of theory are shown in Fig. 4a–g respectively, where the numbering of the atoms are defined and the values mentioned are in Å. The optimized structures of all the other complexes are shown in Figs. S1–S6 in the supporting information. For convenience, the five most stable GD conformers are represented as GDC1, GDC2, GDC3, GDC4 and GDC5. The optimized structural parameters (selected values) of the most stable conformers of bare and hydrated GD along with the available experimental results [13,42,43] are given

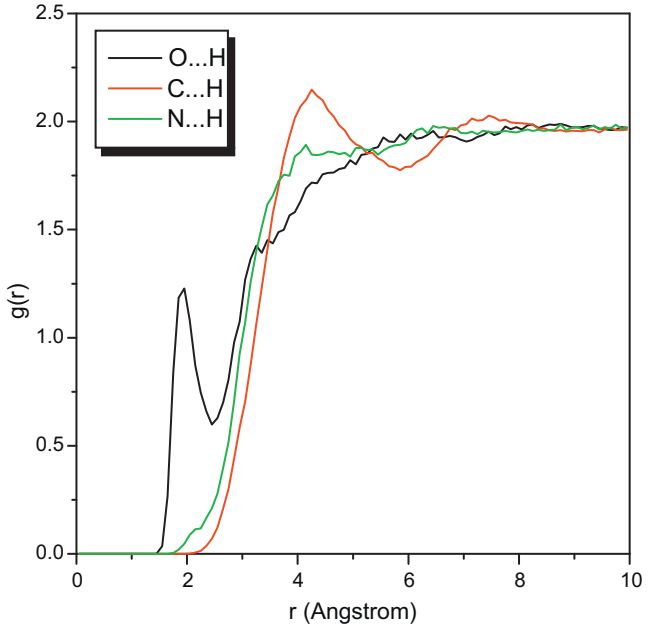

Fig. 2. Radial distribution functions of the GD in water.

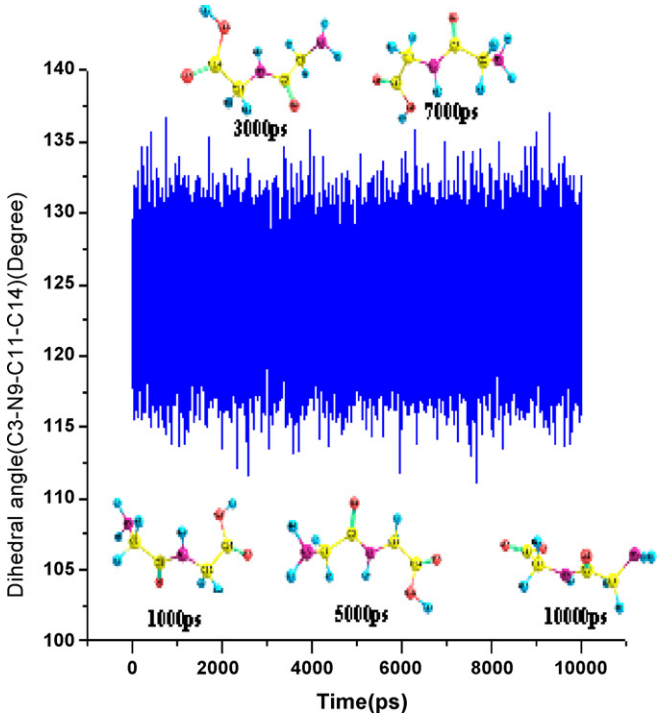

Fig. 1. The conformational changes of GD over 10 ns using MD simulations.

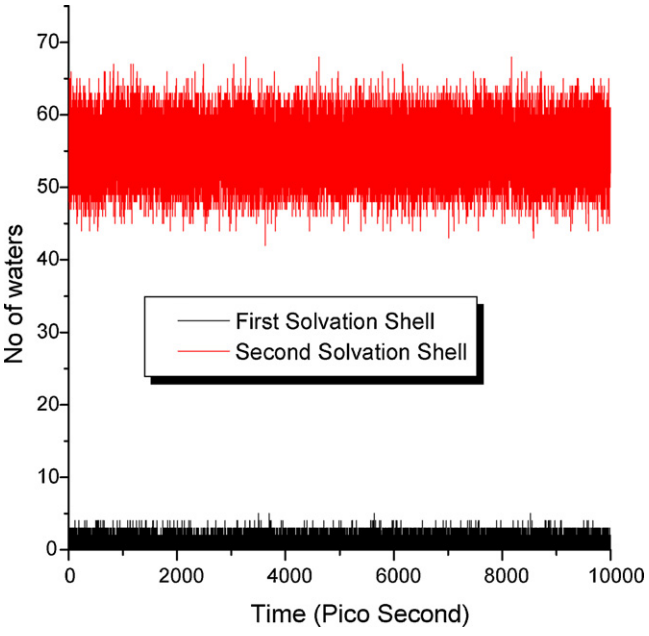

Fig. 3. Time progression of the number of water molecules in 1st and 2nd shell of GD.

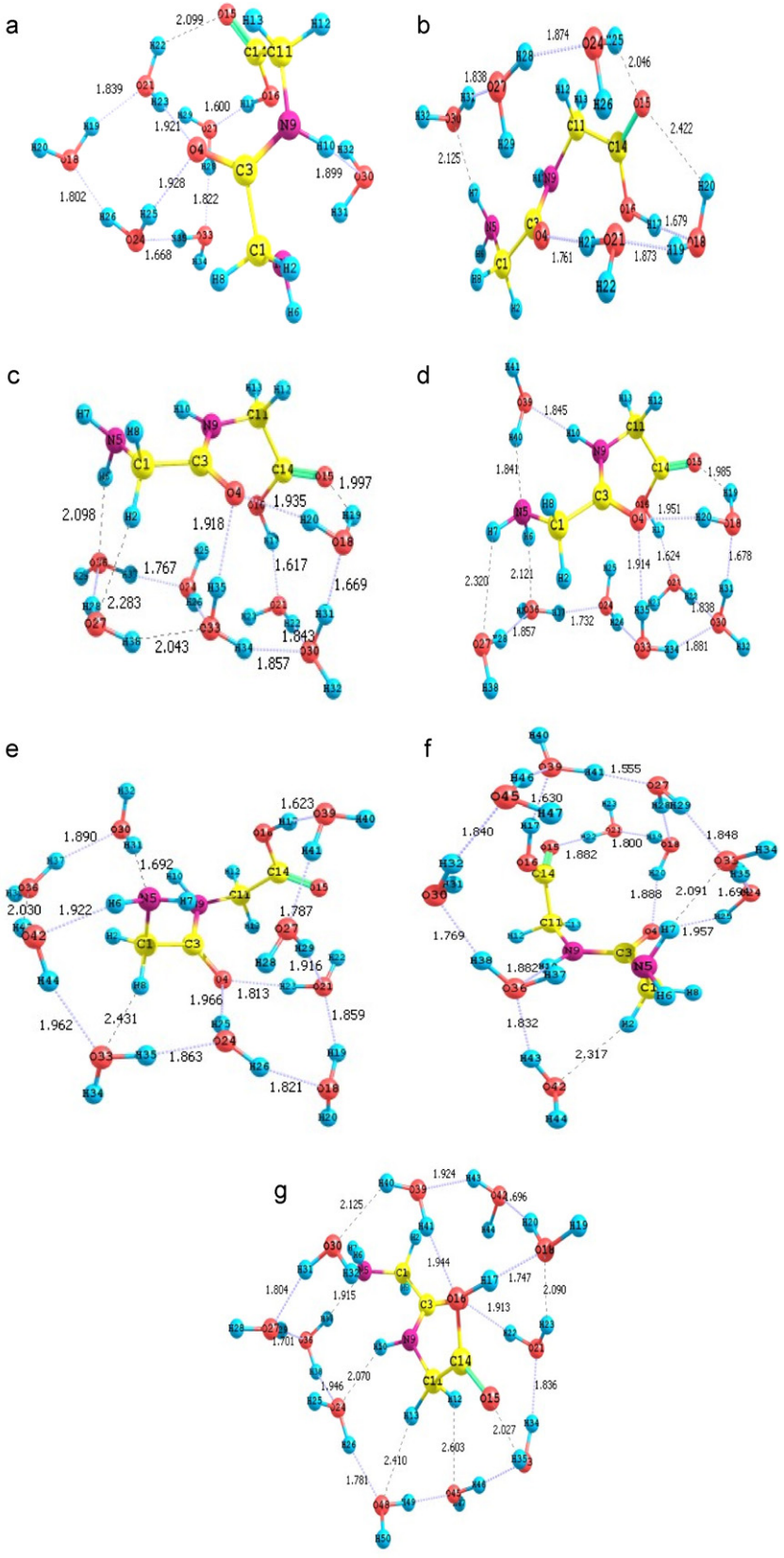

Fig. 4. (a)–(g) Optimized structures of the most stable GD···$(W)_n$ $n = 5–11$ complexes.

in Table 2. The calculated amide plane bond parameters (C1—C3, C3═O, C3—N9 and N9—H10) which are the key factors for the investigation of the peptide molecules [44] are comparable with the previous theoretical results [21]. It is interesting to note that the calculated C14—C11 bond length, N5C1C3 and C3N9C11 bond angles of GD agree well with the experimental values. The C14C11N9 bond angle of GD is larger by 6.21° [42], 4.31° [13] and 3.71° [43] from the experimental values. This difference is due to

Table 2
Selected geometrical parameters (bond length R (in Å), bond angle θ (in degree)) for the most stable conformers of bare (GDC1) and hydrated GD···$(W)_n$ n = 5–10 complexes calculated at B3LYP/6-311G** level of theory. For labeling of atoms refer Fig. 4a–g.

Parameter	Bare GD			Hydrated complexes					
	GDC1			GD+5W	GD+6W	GD+7W	GD+8W	GD+9W	GD+10W
	B3LYP	Experimental		GDC1	GDC5	GDC3	GDC3	GDC5	GDC5
C14—O16	1.352	1.243[a]	1.246[b]	1.319	1.326	1.326	1.326	1.320	1.326
C14—O15	1.202	1.257[a]	1.248[b]	1.219	1.213	1.212	1.213	1.216	1.214
C14—C11	1.519	1.518[a]	1.529[b]	1.522	1.532	1.530	1.528	1.534	1.528
C11—N9	1.437	1.446[a]	1.452[b]	1.447	1.454	1.448	1.451	1.455	1.449
C3—N9	1.358	1.326[a]	1.333[b]	1.338	1.344	1.341	1.340	1.347	1.344
C3—O4	1.218	1.238[a]	1.221[b]	1.241	1.242	1.242	1.244	1.243	1.242
C3—C1	1.531	1.515[a]	1.525[b]	1.525	1.531	1.525	1.524	1.518	1.528
C1—N5	1.467	1.474[a]	1.472[b]	1.460	1.476	1.468	1.469	1.481	1.480
N9—H10	1.009	–		1.016	1.026	1.018	1.025	1.021	1.027
O15—C14—O16	123.04	126.6[a]	126.2[b]	124.52	125.17	124.36	124.15	124.95	123.72
C11—C14—O16	113.61	115.6[a]	115.9[b]	115.04	112.63	113.58	114.16	111.90	112.76
C11—C14—O15	123.36	118.0[a]	117.9[b]	120.44	122.17	122.04	121.67	123.14	123.51
N9—C11—C14	116.11	109.1[a]	111.8[b]	115.99	112.84	114.93	115.12	111.54	114.45
C3—N9—C11	121.96	121.6[a]	109.9[b]	123.59	120.51	123.34	121.15	121.62	121.55
O4—C3—N9	124.39	123.0[a]	122.0[b]	124.50	122.95	123.47	122.26	123.13	122.63
C1—C3—O4	121.24	120.3[a]	124.6[b]	120.99	120.77	121.75	118.93	120.79	120.94
C1—C3—N9	114.36	116.8[c]		114.50	116.28	114.77	118.81	116.01	116.42
N5—C1—C3	113.10	113.3[a]	114.4[b]	110.71	110.75	111.85	116.20	108.97	110.59
C3—N9—H10	115.65	–		113.62	117.15	113.67	120.67	116.74	117.94
H10—N9—C11	121.65	–		120.95	115.46	122.99	117.75	117.65	118.98

[a] Taken from Ref. [42].
[b] Taken from Ref. [13].
[c] Taken from Ref. [43].

the presence of lone pair electrons in nitrogen atoms which cause difficulty in determining the bond angles. All the other geometrical parameters are comparable with the experimental results.

The geometries of the α-carbons are important since they play a crucial role in the overall structure of protein [25,44]. The formation of all hydrated complexes characterizes an elongation of C14—$C^{\alpha 2}$ (C atom belongs to second glycine), $C^{\alpha 2}$—N9 and N5—$C^{\alpha 1}$ (C atom belong to first glycine) bond lengths which range from 1.519 to 1.534, 1.447 to 1.454 and 1.467 to 1.480 Å respectively. The shortening and hence strengthening of C3—$C^{\alpha 1}$ bond is observed. Compared to $C^{\alpha 2}$, larger variation in the $C^{\alpha 1}$ bond angles are noticed. This difference can be explained by the fact that there is a significant difference between the N of the amine group of the first glycine and N of the plane (previously of amine group) of the second glycine and similarly with the carboxyl carbon [44]. It appears as though there also could be H-bond like attractive forces between the amide plane hydrogen (H10) and the carboxylic oxygen atom (O16) (2.508–3.037 Å) as well as between the amide plane oxygen (O4) and one of the hydrogens of the second glycine α-carbon (H12) (2.340–3.228 Å). These bonds are considered as weak H-bonds in peptide system [25,45]. Overall elongation of C3═O4 and shortening of C3—N9 bonds were observed in the solvated GD complexes. This is due to the delocalization of the N lone pair with the C═O double bond, which results in "N═C—O" resonance structure and is stabilized by the O—H bond. Thus the partial double bond character of the C═N bond is increased. The H-bonding interaction at N9—H10 varies from 1.766 to 2.070 Å and does not influence the C3═O4 bond, because of the rigidity of the C3—O9 bond. In the hydrated complexes, N—H···O H-bonds with distances ranging from 1.824 to 2.133, 1.846 to 2.106, 1.766 to 2.098, 1.787 to 2.32, 1.028 to 2.097, 1.811 to 2.262 and 2.07 Å are observed in GD···$(W)_n$ n = 5–11 complexes respectively. In addition to the conventional H-bonds, some non-traditional bonds [46] (C—H···O type) are observed with bond lengths ranging from 2.114 to 2.603 Å in the hydrated complexes.

Table 3 lists the total energy, interaction energy, dipole moment and the torsional angles for the hydrated GD···$(W)_n$ n = 5–10 complexes calculated at B3LYP and B3PW91 methods with 6-311G** basis set. A surprising sensitivity of energy and increase in the stability of the molecular systems are noticed with increasing degree of hydration. Previous studies [9,47–49] reported that as the number of water molecules in the water cluster increases, the 'more solvated' structure becomes the global minimum. Our previous work regarding the molecular dynamics and DFT studies of the incremental solvation effect on Glycine [50] with one to nine water molecules by constructing the hydration shell around the Glycine also predicted the same result. In the most stable GDC1 and GDC3 of GD···$(W)_5$ complexes, two water molecules associate with carboxylic acid group through H-bonding with distances 1.629 and 2.046 Å and 1.679 and 2.042 Å respectively. Both the structures have originated due to the interaction of water molecules one at carboxylic, one at amine groups further complexed by an addition of three water molecules which act as a bridge between amine and carboxylic groups. Even though, GDC3 is the energitical pair of GDC1, it possesses slightly higher interaction energy (difference is 0.03 kcal/mol). This is due to the presence of an additional H-bond in GDC3. The next and lesser stable structures are having interaction energies −44.37 and −30.12 kcal/mol respectively at B3LYP/6-311G** level of theory. The B3PW91 method predicts the interaction energy for the above two structures as −40.79 and −26.66 kcal/mol respectively. In GD···$(W)_6$ complexes, the lowest energy species (GDC5) emerges with five H-bonds with distances ranging from 1.6 to 2.099 Å. Our calculations on GD conformers with seven water molecules indicate that in the most stable structure (GDC3), the three water molecules prefer to make strong H-bonds to the three hydrogen atoms available at amine, α-carbon and carboxylic groups respectively. Between the two water molecules which make H-bonds with C═O oxygen, one water acts as a bridge between the C═O and carboxylic oxygens. The other two water molecules bind to the available water–water chain. The stability order predicted by B3LYP (GDC3 > GDC1 > GDC2 > GDC5 > GDC4) is contradicted by B3PW91 (GDC3 > GDC1 > GDC2 > GDC4 > GDC5). Only 1.26 kcal/mol energy difference is noticed between the two structures (GDC4 and GDC5) which cause the change in order of stability. The increase in water molecules enhances the H-bonds between the water molecules which also limit the flexibility of water cluster. In GD···$(W)_8$

Table 3
Total energy E_{tot} (in Hartree), interaction energy E_{int} (in kcal/mol), dipole moment μ_m (in debye) and torsional angles Φ and Ψ (in degrees) for the hydrated GD···$(W)_n$ n = 5–10 complexes calculated at B3LYP/6-311G** and B3BW91/6-311G** levels of theory.

Parameter	GDC1		GDC2		GDC3		GDC4		GDC5	
	B3LYP	B3PW91	B3LYP	B3PW91	B3LYP	B3PW91	B3LYP	B3PW91	B3LYP	B3PW91
GD+5W										
$-E_{tot}$	874.939	874.592	874.571	874.572	874.939	874.592	874.907	874.562	874.931	874.584
$-E_{int}$	47.93	39.22	35.99	32.05	47.96	43.92	30.12	26.66	44.37	40.79
μ_m	3.774	3.770	3.333	3.529	3.821	3.789	4.836	4.749	5.195	5.203
Φ	65.21	65.05	91.22	96.06	65.23	64.98	91.39	93.76	−101.61	−103.84
Ψ	−22.05	−21.78	6.62	5.19	−21.78	−21.80	7.66	8.13	−54.05	−52.83
GD+6W										
$-E_{tot}$	951.394	951.003	951.398	951.020	951.392	951.016	951.399	951.021	951.415	951.036
$-E_{int}$	49.84	44.11	55.44	50.95	49.66	45.88	50.31	45.58	64.40	60.74
μ_m	9.974	4.020	2.612	2.700	2.870	2.788	2.246	2.619	3.387	3.306
Φ	82.15	83.41	114.07	113.39	84.43	86.39	95.24	98.88	−60.25	−60.43
Ψ	10.84	10.71	−58.25	−55.26	14.41	14.65	10.89	9.62	−68.01	−68.13
GD+7W										
$-E_{tot}$	1027.885	1027.476	1027.867	1027.458	1027.890	1027.480	1027.863	1027.456	1027.864	1027.454
$-E_{int}$	69.53	51.46	63.63	58.73	[a]	[a]	58.48	53.49	60.30	54.59
μ_m	3.370	3.317	4.129	4.134	3.119	3.066	1.570	1.397	4.835	4.679
Φ	59.36	59.10	97.41	98.73	61.48	61.26	129.00	130.94	170.80	−65.11
Ψ	0.26	−0.16	−50.95	−48.56	15.22	14.94	17.34	15.98	−96.71	−97.02
GD+8W										
$-E_{tot}$	1104.329	1103.892	1104.341	1103.901	1104.352	1103.912	1104.332	1103.894	11 04.345	1103.908
$-E_{int}$	66.03	61.12	67.14	61.02	[a]	[a]	66.08	60.66	79.32	73.54
μ_m	6.561	6.430	3.615	3.720	1.698	1.687	2.988	2.811	2.302	3.580
Φ	124.98	126.56	102.17	104.87	58.62	58.46	145.67	145.72	−59.55	−65.44
Ψ	2.01	0.70	5.74	4.96	20.81	22.12	7.81	6.43	−69.54	−51.45
GD+9W										
$-E_{tot}$	1180.812	1180.341	1180.813	1180.343	1180.800	1180.329	1180.792	1180.323	1180.814	1180.343
$-E_{int}$	78.44	72.67	79.88	73.39	[a]	[a]	71.60	66.15	84.78	77.97
μ_m	4.976	4.846	2.7802	2.766	6.000	6.075	4.925	4.952	5.715	5.602
Φ	142.43	141.97	64.57	64.50	55.29	58.46	108.86	111.20	−74.20	−75.03
Ψ	4.80	4.66	6.02	5.51	64.15	22.11	72.05	69.78	−66.88	−65.10
GD+10W										
$-E_{tot}$	1257.284	1256.782	1257.283	1256.781	1257.265	1256.763	1257.267	1256.766	1257.290	1256.788
$-E_{int}$	92.75	86.03	93.18	85.65	[a]	[a]	81.20	74.36	97.77	90.80
μ_m	3.612	3.496	3.507	3.390	4.892	4.850	10.294	10.5075	3.368	3.551
Φ	64.40	64.00	62.97	62.84	93.62	96.86	126.90	128.05	−82.61	−84.30
Ψ	28.00	27.85	27.71	27.58	60.63	56.34	69.83	67.59	−72.50	−72.18

[a] Did not converge

complexes, the water molecules make more number of H-bonds with NH_2 compared to COOH. Both the DFT methods predict the same order of stability as GDC3 > GDC5 > GDC2 > GDC4 > GDC1. In the minimum energy structure of GD···$(W)_9$ complex (GDC5), the water molecules are distributed and strengthens the water–water and GD–water interactions by forming water bridges. In this structure, the water molecules have avoided the N—H and $C^{\alpha 2}$ moiety. The least stable structure arises due to the formation of cluster of water molecules through water–water binding with seven H-bonds (1.725–2.173 Å) by exposing the carboxylic group. In the minimum energy structure of GD···$(W)_{10}$ complex (GDC5), the water molecules form a concave shape in which the GD is embedded, although not fully solvated with both the amine and carboxyl groups participating in H-bonds with water cluster. Here, the carboxyl clustering motif dominates with some small (only 2) water density near the amino group. The ten water molecules link the water ring to the GD by forming six H-bonds. Even though, the remaining four water molecules are not forming direct H-bonds with GD, the water–water binding play a vital role in the stability of the complex with interaction energy −97.77 and −90.8 kcal/mol at B3LYP and B3PW91 level of theories respectively. The lowest energy conformer (GDC4) of GD···$(W)_{11}$ complex appears to be fully solvated (i.e.) completely surrounded by water molecules [48,49]. The lesser number of H-bonds at N—H group compared to the carboxyl group is observed. This may be due to the partial negative charge of O atom of carboxyl group which diminishes the electrostatic potential in the vicinity of the NH, making it a less inviting target to an incoming proton acceptor group. In most cases, interaction at the amino group is higher than at carbonyl. This is due to the presence of cyclic H-bonding interactions in GD. This is well supported by the previous theoretical result [21]. The five most stable conformers of GD predicted by QM and MD simulations with their energy are shown in Fig. 5a. In order to investigate the effect of solvation with 10 water molecules on the conformers predicted by MD, the quantum chemical calculations were carried out at B3LYP/6-311G** level of theory. The conformational changes in the both QM and MD predicted hydrated complexes with their energies (see Fig. 5b) show that QM is capable of predicting the energetically favorable conformers.

In hydrogen bonded complexes, the electrostatic effects such as dipole moment play an important role [51]. It is believed that the energetics of H-bond formation of peptide is directly correlated with its dipole moment [52]. The calculated dipole moment values (see Table 3) of the GD conformers are not as much close to the earlier results [53] as hoped for. A substantial enhancement of dipole moment has been noticed for all the complexes except a few. The augmentation of dipole moment is due to the influence of the polar environment. The dipole moment of the solute molecule induces a dipole moment in each solvent molecule that adds to permanent dipole which increases the net dipole moment of the hydrated structures. The earlier studies [54,55] also show that the dipole moment is increased during the formation of H-bonds in complex. Among all hydrated complexes, the maximum dipole moment 10.294 debye is observed for GDC4 of GD···$(W)_{10}$ complex. Among GD···$(W)_5$ complexes, the maximum dipole moment value 5.195 debye is observed for GDC5 in which water molecules form a

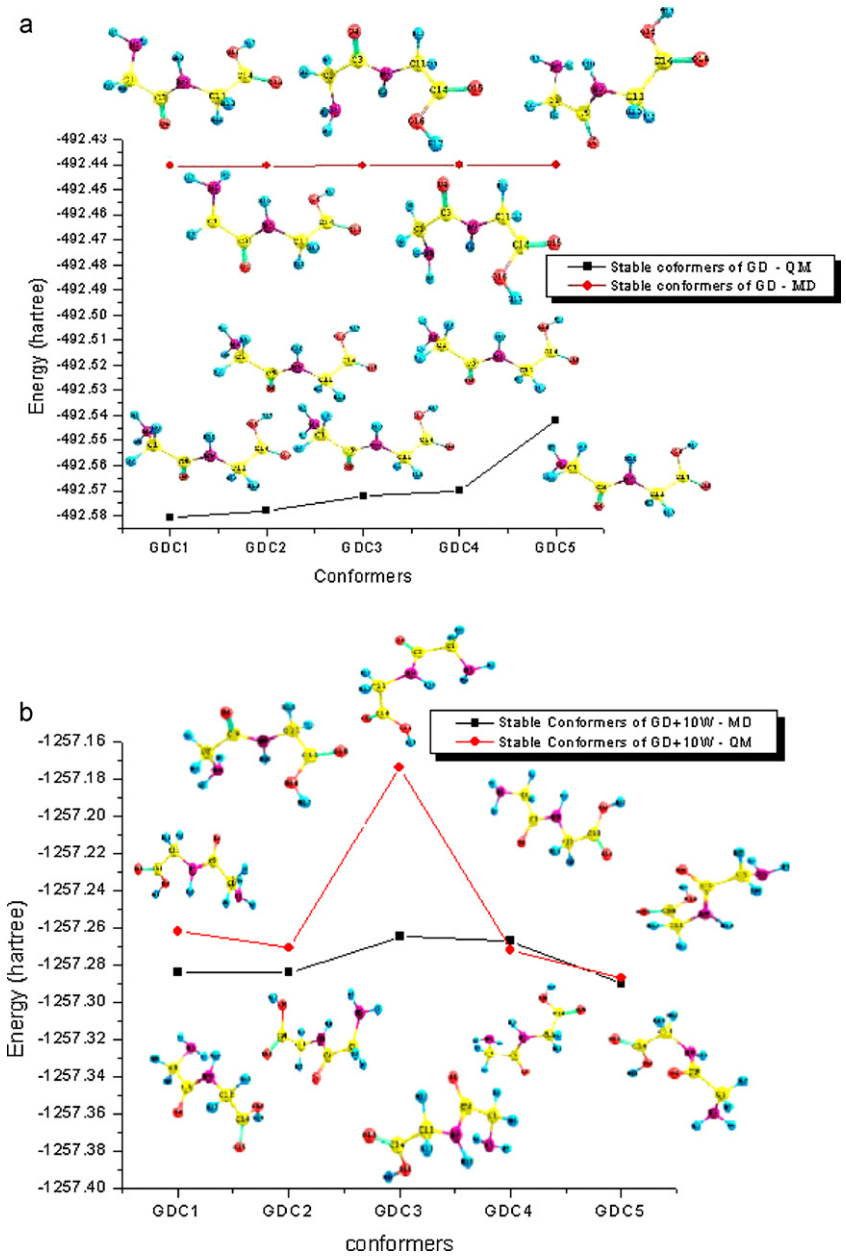

Fig. 5. (a) The most stable GD conformers predicted by QM and MD with their energy (in Hartrees). (b) The QM and MD predicted GD conformers with 10 water molecules and their energy (in Hartrees) (the water molecules are removed for clarity).

ring structure with stronger water–water binding. The same trend is observed for remaining complexes in which in addition to the GD–water H-bonding, the tighter and stronger water–water binding also exist which leads to comparatively larger dipole moments.

3.2.2. Topological analysis

The calculated values of charge density ($\rho(r)$), Laplacian of charge density ($\nabla^2\rho(r)$) and ellipticity (ε) for the most stable complexes calculated at B3LYP/6-311G** level of theory for GD···$(W)_n$ $n = 5–10$ complexes are listed in Table 4 and these values for all the other complexes are given in Table S1 in the supporting information. The H17···O18 bond in GDC1 of GD···$(W)_6$ complex is found to be relatively short (1.627 Å) and $\rho(r)$ and $\nabla^2\rho(r)$ at pcb are observed to be 0.056 and 0.126 a.u. respectively. The minimum $\rho(r)$ value of 0.008 a.u. is observed for GDC4 of GD···$(W)_7$ complex between the twelfth hydrogen of GD and oxygen atom of water. The calculated Laplacian density also follows the same trend. In the most stable complex (GDC5) of GD···$(W)_{10}$ complex, the maximum charge density of 0.053 a.u. is observed between hydrogen atom H17 of carboxylic group and the water molecule which leads to the strong H-bond with bond length of 1.630 Å. In general, the strong bonds are associated with maximum electron density and higher structural stability.

Fig. 6 plots a graph for the H-bond length of the strong O—H···O and N—H···O interactions observed in the 10 water complexes of the conformers predicted by QM and MD. In these complexes, the hydrogen bond lengths for the O—H···O and N—H···O interactions vary between 1.63 and 1.903 Å and 1.811 and 2.104 Å respectively for the QM predicted conformers. At the same time, these values vary between 1.76 and 1.938 Å and 1.842 and 2.137 Å respectively for the conformers predicted by MD. In both the cases, the homonuclear interactions are found to be marginally stronger than the heteronuclear interactions. Another property studied at bcp is bond ellipticity. The magnitude of the ellipticity value for the H12···O_W

Table 4
Hydrogen bond length R (Å), electron density $\rho(r)$ (in a.u.), Laplacian of electron density $\nabla^2\rho$ (in a.u.) and ellipticity ε involved in hydrogen bonds in the most stable GD···$(W)_n$ n = 5–10 complexes calculated at B3LYP/6-311G** level of theory. For labeling of atoms refer Fig. 4a–g.

Species		Bond	R (Å)	ρ (r)	$\nabla^2\rho$	ε
GD+5W	GDC1	H23···O4	1.761	0.035	0.117	0.014
		H17···O18	1.679	0.050	0.122	0.030
		H25···O15	2.046	0.020	0.071	0.029
		H7···O30	2.125	0.018	0.063	0.087
GD+6W	GDC5	H10···O30	1.899	0.031	0.098	0.040
		H17···O27	1.600	0.060	0.128	0.050
		H23···O4	1.921	0.024	0.084	0.021
		H25···O4	1.928	0.027	0.086	0.044
GD+7W	GDC3	H6···O36	2.098	0.018	0.065	0.086
		H2···O27	2.283	0.015	0.046	0.045
		H35···O4	1.918	0.026	0.087	0.057
		H20···O4	1.935	0.024	0.084	0.003
		H17···O21	1.617	0.057	0.126	0.050
		H19···O15	1.997	0.021	0.079	0.038
GD+8W	GDC3	H19···O15	1.985	0.022	0.085	0.050
		H20···O4	1.951	0.023	0.090	0.010
		H35···O4	1.914	0.027	0.097	0.063
		H17···O21	1.624	0.057	0.141	0.052
		H6···O36	2.121	0.019	0.064	0.096
		H7···O27	2.320	0.013	0.047	0.285
		H40···N5	1.841	0.041	0.100	0.021
GD+9W	GDC5	H31···N5	1.692	0.057	0.091	0.017
		H6···O42	1.922	0.029	0.095	0.034
		H8···O33	2.431	0.011	0.035	0.141
		H25···O4	1.966	0.024	0.078	0.047
		H23···O4	1.813	0.032	0.108	0.039
		H17···O39	1.623	0.055	0.130	0.028
GD+10W	GDC5	H17···O39	1.630	0.053	0.097	0.062
		H10···O36	1.882	0.032	0.134	0.018
		H2···O42	2.317	0.013	0.043	0.052
		H25···O4	1.957	0.025	0.083	0.046
		H7···O33	2.091	0.019	0.066	0.065
		H20···O4	1.888	0.026	0.094	0.036
		H22···O15	1.882	0.026	0.096	0.036

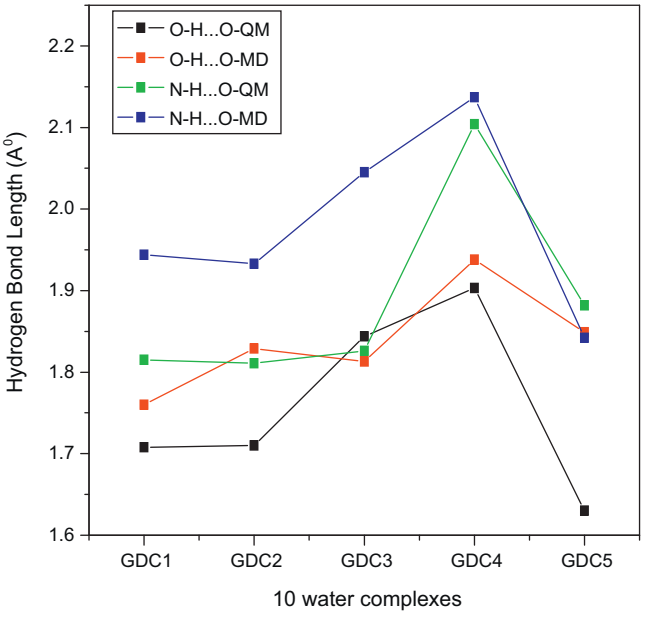

Fig. 6. Graph for the strong O—H···O and N—H···O interactions present in the 10 water complexes of the conformers predicted by QM and MD.

Table 5
Electron donor orbital, electron acceptor orbital and their corresponding stabilization energies $E^{(2)}$ (in kcal/mol) of the most stable GD···$(W)_n$ n = 5–10 complexes calculated at B3LYP/6-311G** level of theory. For labeling of atoms refer Fig. 4a–g.

Species		Donor	Acceptor	$E^{(2)}$
GD+5W	GDC1	LP(1)O4	BD*(1)O21—H23	8.56
		LP(1)O18	BD*(1)O16—H17	27.24
		LP(1)O15	BD*(1)O24—H25	1.83
		LP(1)O30	BD*(1)N5—H7	3.69
GD+6W	GDC5	LP(1)O30	BD*(1)N9—H10	11.53
		LP(1)O27	BD*(1)O16—H17	35.84
		LP(1)O4	BD*(1)O21—H23	4.47
		LP(1)O4	BD*(1)O24—H25	5.61
GD+7W	GDC3	LP(1)O36	BD*(1)N5—H6	4.44
		LP(1)O27	BD*(1)C1—H2	3.65
		LP(2)O4	BD*(1)O33—H35	2.58
		LP(1)O4	BD*(1)O18—H20	4.35
		LP(1)O21	BD*(1)O16—H17	33.86
		LP(1)O15	BD*(1)O18—H19	1.71
GD+8W	GDC3	LP(1)O15	BD*(1)O18—H19	1.79
		LP(1)O4	BD*(1)O18—H20	4.05
		LP(1)O4	BD*(1)O33—H35	3.50
		LP(1)O21	BD*(1)O16—H17	33.15
		LP(1)O36	BD*(1)N5—H6	4.42
		LP(1)O27	BD*(1)N5—H7	0.79
		LP(1)N5	BD*(1)O39—H40	19.25
GD+9W	GDC5	LP(1)N5	BD*(1)O30—H31	32.89
		LP(1)O42	BD*(1)N5—H6	11.00
		LP(1)O33	BD*(1)C1—H8	0.77
		LP(1)O4	BD*(1)O24—H25	4.85
		LP(1)O4	BD*(1)O21—H23	6.63
		LP(1)O39	BD*(1)O16—H17	32.14
GD+10W	GDC5	LP(1)O39	BD*(1)O16—H17	30.17
		LP(1)O36	BD*(1)N9—H10	12.72
		LP(1)O42	BD*(1)C1—H2	2.69
		LP(1)O4	BD*(1)O24—H25	4.22
		LP(1)O33	BD*(1)N5—H7	4.77
		LP(1)O4	BD*(1)O18—H20	4.47
		LP(1)O15	BD*(1)O21—H22	2.40

bond in GDC4 of GD···$(W)_7$ complex is found to be higher and greater than one (1.408) as compared to other hydrated complexes which is the indication for the system to approach a bifurcation point in which the atoms bond to different partners and a conformational change is expected. Further, smaller ellipticity value of 0.002 is observed for GDC2 of GD···$(W)_7$ complex.

3.2.3. NBO analysis

Electron donor orbital (i), electron acceptor orbital (j) and their stabilization energies $E^{(2)}$ corresponding to prominent interactions found in the most stable conformers of the GD···$(W)_n$ n = 5–10 complexes calculated at B3LYP/6-311G** level of theory are listed in Table 5 and these values for all the other complexes are given in Table S2 in the supporting information. In general, the interactions where oxygen of water offers lone pairs to the O—H antibond orbital of GD are stronger, and $E^{(2)}$ lies within the range of 15.01–53.07 kcal/mol, but the interaction where the oxygen of GD offers lone pairs to the O—H antibonding orbital is lesser which lies within the range of 0.83–12.56 kcal/mol. This indicates that the oxygen of water is liable to offer electrons to GD than the oxygen of GD, and the formed hydrogen bonding interaction is strong and the corresponding complex is stable [56]. The interactions between the oxygen lone pairs of water and C—H and N—H antibonding orbital of GD also exist in water interacting complexes with stabilization energies ranging from 0.34 to 6.12 and 0.70 to 19.08 kcal/mol respectively. The N9—H10···O_W interaction in GDC4 of GD···$(W)_{11}$ complex has the stabilization energy of 3.69 kcal/mol which is 9.03 kcal/mol lesser than the most stable GD···$(W)_{10}$ complex (GDC5). The reason behind this type of weak N—H···O hydrogen

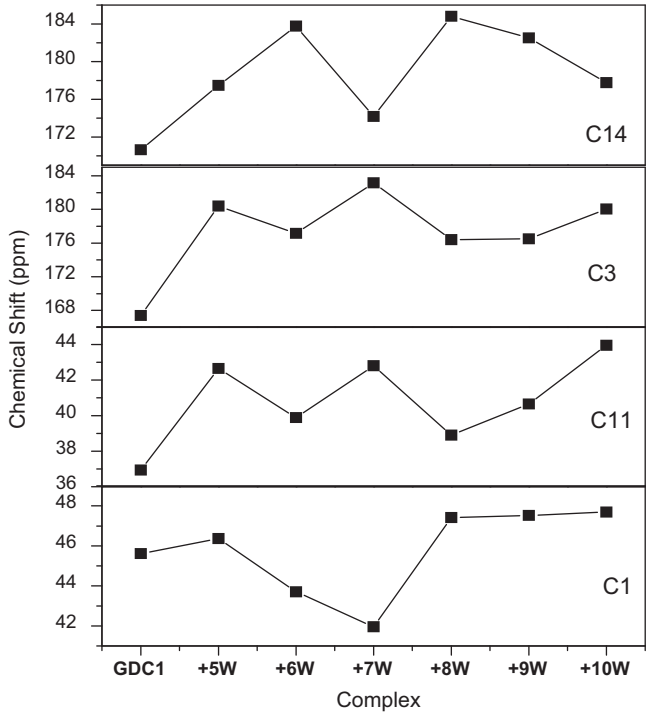

Fig. 7. Variation of chemical shift values (in ppm) of the carbon atoms (C3, C14, C1 and C11) for the most stable conformer GDC1 of bare GD and its hydrated complexes.

bond energies is the electrostatic in origin, that is, during the formation of the H-bond, the conformer places the carbonyl 'O' in the close proximity of the NH that is to be donated to the other proton acceptor or another peptide. While this association is not properly disposed to form an internal H-bond of any consequence, the partial negative charges on the carbonyl 'O' act as a barrier that impedes the opportunity of the proton acceptor [24].

3.2.4. Nuclear shielding and chemical shift

The NMR chemical shift is a sensitive reporter of the peptide secondary structure and its solvation environment, and it is potentially rich with information about both backbone dihedral angles and hydrogen bonding [16,57]. Since the oxygens are directly bonded to carbons, the changes in the electron density around the oxygens due to hydrogen bonding can be monitored indirectly via changes in the NMR chemical shift of the adjacent carbons. All the calculated chemical shifts were referenced to the tetramethylsilane (TMS) and are presented in Table S3 in the supporting information. The chemical shifts of bare GD are found to agree with the experimentally calculated values [13,16]. The carbonyl carbon (C14) has maximum chemical shift values in all the conformations of GD. This is due to the presence of two nearby electronegative oxygen atoms which attract the electron clouds of the carbon atom toward them. This leads to deshielding of carbon atom and the net result is increase in the chemical shift value. The chemical shift values of C=O carbon atom is ranging from 166.20 to 168.73 ppm which has the effect of only one oxygen atom attached to it. The changes in C1 and C11 chemical shift values confirm the changes in the conformations of GD. The calculated chemical shift values of the solvated complexes show that the N-terminal C^{α} carbon (C1) is more sensitive to the structural changes (41.95–48.58 ppm) than the C-terminal (C11) (38.04–44.97 ppm) counterpart.

The calculated chemical shift values of the carboxylic carbon (C14) are in accordance with the experimental values in the solvated state (179.19 ppm) [16]. In GD···$(W)_n$ $n = 6$ and 9 complexes, for the first three conformations, the C14 has the maximum chemical shift values. In both the cases, the C14 of the GDC2 register the minimum chemical shift values (176.46 and 179.81 ppm respectively). In addition to this, the maximum chemical shift values observed for C14 in the GDC2 of GD···$(W)_5$, GDC1 and GDC3 of GD···$(W)_8$ and GDC4 of GD···$(W)_{11}$ complexes show that the terminal carboxylic carbon reflects the structural changes upon solvation. Fig. 7 shows the variation of chemical shift values of the carbon atoms C3, C14 and C1, C11 for the most stable conformer GDC1 of bare GD and its hydrated complexes. In all the remaining, including GD···$(W)_n$ $n = 7$ and 10 complexes, C=O carbon has the maximum chemical shift values which reflects the changes in the electronic environment due to H-bonding.

4. Conclusion

The MD studies reveals that the GD interacts well with the surrounding water molecules and an average of two and sometimes four water molecules are found to have active interaction with GD. The DFT methods were used to probe the sequential hydration of the five lowest energy conformers of GD with 5–10 water molecules which provides an excellent point of entry to add considerable insight into the structure and solvation regarding the hydration of proteins. The influence of water molecules on the structure and stability of the hydrated GD complexes has been analyzed. As the number of water molecules increases, the more solvated complex becomes the global minimum. It is observed that the GD interacts with water molecules through H-bonding and the geometry is altered. Because of the presence of cyclic hydrogen bonding interactions in GD, the interactions at the amino group is higher than at carbonyl. The vibrational frequencies were computed to confirm all the optimized structures to be local energy minima. The presence and strength of H-bonds have been identified and analyzed through the interaction energies. The calculated topological parameters show the existence of strong H-bonds associated with maximum electron density and higher stability. The NBO analysis has revealed the strong intermolecular interactions in the hydrated complexes, which lead to charge transfer from the Y atom lone pairs to the σ^*(X—H) antibonds. The calculated NMR chemical shift values for the carbon atoms confirm that the terminal carboxylic group undergoes significant structural repositioning in the solvated state and the $C^{\alpha 1}$ chemical shift is more sensitive to the structural changes than its C-terminal counterpart.

Acknowledgment

The authors Dr. R. Kanakaraju and Mrs. B. Yogeswari gratefully acknowledge the University Grants Commission, New Delhi, India for the financial support in the form of Major Research Project (No.: 40-436/2011 (SR)).

Appendix A. Supplementary data

Supplementary data associated with this article can be found, in the online version, at doi:10.1016/j.jmgm.2012.02.002.

References

[1] P. Hobza, P.Z. Havlas, Blue-shifting hydrogen bonds, Chem. Rev. 100 (2000) 4253–4264.
[2] R.H.G. Garrett, M. Charles, Biochemistry, 2nd ed., Saunders College Publishing, Philadelphia, 1999.
[3] J.C. Dearden, Quantitative structure–property relationships for prediction of boiling point, vapor pressure, and melting point, Environ. Toxicol. Chem. 22 (2003) 1696–1709.
[4] S.P. de Visser, Density functional theory (DFT) and combined quantum mechanical/molecular mechanics (QM/MM) studies on the oxygen activation step in nitric oxide synthase enzymes, Biochem. Soc. Trans. 37 (2009) 373–377.
[5] D. Liu, T. Wyttenbach, P.E. Barran, M.T. Bowers, Sequential hydration of small protonated peptides, J. Am. Chem. Soc. 125 (2003) 8458–8464.

[6] G.A. Jeffrey, An Introduction to Hydrogen Bonding, Oxford University Press, Oxford, 1997.
[7] A. Madhumalar, M. Bansal, Structural insights into effect of hydration and ions on A-tract DNA – a molecular dynamics study, Biophys. J. 85 (2003) 1805–1816.
[8] C.C. Wu, C. Chaudhuri, J.C. Jiang, Y.T. Lee, H.C. Chang, Hydration-induced conformational changes in protonated 2,4-pentanedione in the gas phase, Mol. Phys. 101 (2003) 1285–1295.
[9] C.M. Aikens, M.S. Gordon, Incremental solvation of nonionized and zwitterionic Glycine, J. Am. Chem. Soc. 128 (2006) 12835–12850.
[10] E.L. Eliel, S.H. Wilen, L.N. Mander, Sterochemistry of Organic Compounds, Wiley-Interscience, New York, 1994.
[11] R. Walser, W.F.V. Gunsteren, Viscosity dependence of protein dynamics, Proteins 42 (2001) 414–421.
[12] C. Mattos, Protein–water interactions in a dynamic world, Trends Biochem. Sci. 27 (2002) 203–208.
[13] T. Kameda, N. Takeda, S. Ando, I. Ando, D. Hashizume, Y. Ohashi, Structure of GlyGly peptide in the crystalline state as studied by X-ray diffraction and solid state ^{13}C NMR methods, Biopolymers 45 (1998) 333–339.
[14] G. Sieler, R.S. Stenner, The amide I mode of peptides in aqueous solution involves vibrational coupling between the peptide group and water molecules of the hydration shell, J. Am. Chem. Soc. 119 (1997) 1720–1726.
[15] D. Liu, T. Wyttenbach, C.J. Carpenter, M.T. Bowers, Investigation of noncovalent interactions in deprotonated peptides: structural and energetic competition between aggregation and hydration, J. Am. Chem. Soc. 126 (2004) 3261–3270.
[16] M.P. Bhate, J.C. Woodard, M.A. Mehta, Solvation and hydrogen bonding in alanine- and glycine-containing dipeptides probed using solution- and solid-state NMR spectroscopy, J. Am. Chem. Soc. 131 (2009) 9579–9589.
[17] B. Born, H. Weingartner, E. Brundermann, M. Havenith, Solvation dynamics of model peptides probed by terahertz spectroscopy. Observation of the onset of collective network motions, J. Am. Chem. Soc. 131 (2009) 3752–3755.
[18] G. Fischer, X. Cao, N. Cox, M. Francis, The FT-IR spectra of glycine and glycylglycine zwitterions isolated in alkali halide matrices, Chem. Phys. 313 (2005) 39–49.
[19] Y.A. Abramov, A. Volkov, G. Wu, P. Coppens, Use of X-ray charge densities in the calculation of intermolecular interactions and lattice energies. Application to glycylglycine, DL-histidine, and DL-proline and comparison with theory, J. Phys. Chem. B 104 (2000) 2183–2188.
[20] P. Chaudhuri, S. Canuto, An ab initio study of the peptide bond formation between alanine and glycine: electron correlation effects on the structure and binding energy, J. Mol. Struct. (Theochem) 577 (2002) 267–279.
[21] P. Selvarengan, P. Kolandaivel, Molecular modeling of dipeptide and its analogous systems with water, J. Mol. Model. 10 (2004) 198–203.
[22] O. Makshakova, E. Ermakova, Computational study of hydrogen-bonding complex formation of helical polypeptides with water molecule, J. Mol. Struct. (Theochem) 942 (2010) 7–14.
[23] H. Hugosson, A. Laio, P. Maurer, U. Rothlisberger, A comparative theoretical study of dipeptide solvation in water, J. Comput. Chem. 27 (2006) 672–683.
[24] S. Scheiner, The strength with which a peptide group can form a hydrogen bond varies with the internal conformation of the polypeptide chain, J. Phys. Chem. B 111 (2007) 11312–11317.
[25] C.D. Keefe, J.K. Pearson, Ab initio investigations of dipeptide structures, J. Mol. Struct. (Theochem) 679 (2004) 65–72.
[26] F. Elmi, N.L. Hadipour, A study on the intermolecular hydrogen bonds of alpha-glycylglycine in its actual crystalline phase using ab initio calculated ^{14}N and ^{2}H nuclear quadrupole coupling constants, J. Phys. Chem. A 109 (2005) 1729–1733.
[27] S. Scheiner, Cooperativity of multiple H-bonds in influencing structural and spectroscopic features of the peptide unit of proteins, J. Mol. Struct. 976 (2010) 49–55.
[28] Z. Yan, Y. Li, X. Wang, J. Dan, J. Wang, Effect of glycyl dipeptides on the micellar behaviour of gemini surfactant: a conductometric and fluorescence spectroscopic study, J. Mol. Liquids 161 (2011) 49–54.
[29] T.C. Cheam, Normal mode analysis of Glycine Dipeptide in crystal conformation using a scaled ab initio force field, J. Mol. Struct. 274 (1992) 289–309.
[30] W.L. Jorgensen, J. Chandrasekhar, J.D. Madura, M.L. Klein, R.W. Impey, Comparison of simple potential functions for simulating liquid water, J. Chem. Phys. 79 (1983) 926–935.
[31] C.R.W. Guimaraes, G. Barreiro, C. Augusto, F.D. Oliveira, R.B.D. Alencastro, On the application of simple explicit water models to the simulations of biomolecules, Braz. J. Phys. 34 (2004) 126–136.
[32] D.A. Case, T.A. Darden, T.E. Cheatham III, C.L. Simmerling, J. Wang, R.E. Duke, R. Luo, K.M. Merz, B. Wang, D.A. Pearlman, M. Crowley, S. Brozell, V. Tsui, H. Gohlke, J. Mongan, V. Hornak, G. Cui, P. Beroza, C. Schafmeister, J.W. Caldwell, W.S. Ross, P.A. Kollman, Amber 8, University of California, San Francisco, 2004.
[33] A.D. Becke, Density – functional exchange – energy approximation with correct asymptotic behaviour, Phys. Rev. A 38 (1998) 3098–3100.
[34] C. Lee, W. Yang, R.G. Parr, Development of the corre-salvetti correlation energy formulae into a functional of the electron density, Phys. Rev. B 37 (1988) 785–789.
[35] J.P. Predew, Y. Wang, Accurate and simple analytic representation of the electron-gas correlation energy, Phys. Rev. B 45 (1992) 13244–13249.
[36] S.F. Boys, F. Bernardi, The calculation of small molecular interactions by the differences of separate total energies. Some procedures with reduced errors, Mol. Phys. 19 (1970) 553–566.
[37] R.F.W. Bader, Atoms in Molecules: A Quantum Theory, Oxford University Press, Oxford, 1990.
[38] J.R. Cheeseman, G.W. Trucks, T.A. Keith, M.J. Frisch, A comparison of models for calculating NMR Shielding tensors, J. Chem. Phys. 104 (1996) 5497–5509.
[39] M.J. Frisch, G.W. Trucks, H.B. Schlegel, G.E. Scuseria, M.A. Robb, J.R. Cheeseman, V.G. Zakrzewski, J.A. Montgomery Jr., R.E. Stratmann, J.C. Burant, S. Dapprich, J.M. Millam, A.D. Daniels, K.N. Kudin, M.C. Strain, O. Farkas, J. Tomasi, V. Barone, M. Cossi, R. Cammi, B. Mennucci, C. Pomelli, C. Adamo, S. Clifford, J. Ochterski, G.A. Petersson, P.Y. Ayala, Q. Cui, K. Morokuma, N. Rega, P. Salvador, J.J. Dannenberg, D.K. Malick, A.D. Rabuck, K. Raghavachari, J.B. Foresman, J. Cioslowski, J.V. Ortiz, A.G. Baboul, B.B. Stefanov, G. Liu, A. Liashenko, P. Piskorz, I. Komaromi, R. Gomperts, R.L. Martin, D.J. Fox, T. Keith, M.A. Al-Laham, C.Y. Peng, A. Nanayakkara, M. Challacombe, P.M.W. Gill, B. Johnson, W. Chen, M.W. Wong, J.L. Andres, C. Gonzalez, M. Head-Gordon, E.S. Replogle, J.A. Pople, Gaussian03, Revision B.05, Gaussian, Inc., Pittsburgh, PA, 2003.
[40] P. Doruker, I. Bahar, Role of water on unfolding kinetics of helical peptides studied by molecular dynamics simulations, Biophys. J. 72 (1997) 2445–2456.
[41] E. Tang, D.D. Tomoso, N.H. de Leeuw, Hydrogen transfer and hydration properties of $H_nPO_4^{3-n}$ (n=0–3) in water studied by first principles molecular dynamics simulations, J. Chem. Phys. 130 (2009) 234502-1–1234502-9.
[42] H.C. Freeman, G.L. Paul, T.M. Sabine, J.N. Wilson, A neutron diffraction study of perdeutero-α-glycylglycine, Acta Crystallogr. B 26 (1970) 925–932.
[43] A.B. Biswas, E.W. Hughes, B.D. Sharma, J.N. Wilson, The crystal structure of α-glycylglycine, Acta Crystallogr. B 24 (1968) 40–50.
[44] S. Mondal, D.S. Chowdhuri, S. Ghoush, A. Misra, S. Dalai, Conformational study on dipeptides containing phenylalanine: a DFT approach, J. Mol. Struct. (Theochem) 810 (2007) 81–89.
[45] Y.L. Zhao, Y.D. Wu, A theoretical study of beta-sheet models: is the formation of hydrogen-bond networks cooperative? J. Am. Chem. Soc. 124 (2002) 1570–1571.
[46] P. Selvarengan, P. Kolandaivel, Theoretical study of CH···O hydrogen bond in proton transfer reaction of glycine, Int. J. Quantum Chem. 106 (2006) 1001–1008.
[47] R. Ramaekers, J. Pajak, B. Lambie, G. Maes, Neutral and zwitterionic glycine·H_2O complexes: a theoretical and matrix-isolation Fourier transform infrared study, J. Chem. Phys. 120 (2004) 4182–4193.
[48] S.M. Bachrach, T.T. Nguyen, D.W. Demoin, Microsolvation of cysteine: a density functional theory study, J. Phys. Chem. A 113 (2009) 6172–6181.
[49] J.M. Mullin, M.S. Gordon, Alnine: then there was water, J. Phys. Chem. B 113 (2009) 8657–8669.
[50] B. Yogeswari, R. Kanakaraju, A. Abiram, P. Kolandaivel, Molecular dynamics and quantum chemical studies on incremental solvation of glycine, Comput. Theor. Chem. 967 (2011) 81–92.
[51] H. Umeyama, K. Morokuma, The origin of hydrogen bonding. An energy decomposition study, J. Am. Chem. Soc. 99 (1977) 1316–1332.
[52] R.L. Baldwin, Energetics of protein folding, J. Mol. Biol. 371 (2007) 283–301.
[53] R.L. Wright, R.F. Borkman, Ab initio self-consistent field studies of the peptides Gly–Gly, Gly–Ala, Ala–Gly, and Gly–Gly–Gly, J. Phys. Chem. 86 (1982) 3956–3962.
[54] R. Kaschner, G. Seifert, Investigations of hydrogen bonded systems: local density approximations and gradient corrections, Int. J. Quantum Chem. 52 (1994) 957–962.
[55] R. Kanakaraju, P. Kolandaivelu, B.G. Gownlock, Quantum chemical studies of nitrosobuta – 1,3-diene and nitroso styrene molecules, J. Mol. Struct. (Theochem) 577 (2002) 121–129.
[56] L.C. Li, F. Hu, W.F. Cai, A.M. Tian, N.B. Wong, Density functional theory study on hydrogen bonding interaction of luteolin-$(H_2O)_n$, J. Mol. Struct. (Theochem) 911 (2009) 98–104.
[57] H.M. Sulzbach, P.V.R. Schleyer, H.F. Schaefer III, Interrelationship between conformation and theoretical chemical shifts. Case study on glycine and glycine amide, J. Am. Chem. Soc. 166 (1994) 3967–3972.